IEEJ Journal of Industry Applications
Vol.11 No.1 pp.7–19 DOI: 10.1541/ieejjia.21006800

Review Paper

Review of Modeling and Suppression Techniques for Electromagnetic Interference in Power Conversion Systems

Shotaro Takahashi[*a)] Member, Keiji Wada[**] Senior Member
Hideki Ayano[***] Senior Member, Satoshi Ogasawara[****] Fellow
Toshihisa Shimizu[**] Fellow

(Manuscript received June 3, 2021)
J-STAGE Advance published date : Aug. 13, 2021

The switching frequency of power converters is continuing to increase with the demand for their increased power density. Therefore, the frequency band of the electromagnetic interference (EMI) generated by power converters ranges from several kilohertz to 100 MHz or more, thereby increasing the importance of EMI countermeasures in power converters. In addition, with the practical applications of smart grids and microgrids and the introduction of 5G technology, cases wherein power converters and information communication devices are placed in close proximity are continuing to increase. Thus, in societies wherein power converters and information communication devices are highly integrated, it is necessary to ensure electromagnetic compatibility based on a different concept. This paper presents a review on modeling and suppression techniques for the EMI generated by power converters and discusses future prospects in this field.

Keywords: EMI, time-domain modeling, frequency-domain modeling, behavioral modeling, passive EMI filters, active EMI filters

1. Introduction

In terms of efficiency and controllability, power converters that are based on the switching operation of power semiconductor devices continue to expand their range not only to industries and home appliances, but also to automobiles and aircraft. On the other hand, high *dv/dt* or *di/dt* associated with high-speed switching of power semiconductor devices causes electromagnetic interference (EMI) which brings about malfunctions and failures of peripheral devices [(1)–(4)]. Hence, researches have been actively conducted on clarifying the EMI generation mechanism generated by power converters and effective suppression methods [(5)–(10)].

In recent years, wide-bandgap (WBG) power semiconductor devices based on silicon carbide (SiC) and gallium nitride (GaN) have been rapidly promoted into practical use.

WBG power devices realize 10 times or more faster switching than the silicon IGBT (insulated-gate bipolar transistor) that has been widely used in the past. Hence, it is expected that the power converter will achieve dramatically higher efficiency and smaller size [(11)–(15)]. However, further high-speed and high-frequency drive of power converters bring about widening broadband and high-frequency EMI generated by power converters [(16)–(18)]. In addition, discussions have been actively held in the recent years to expand the bandwidth to 150 kHz or less, which is the international standard for EMI generated by power converters. With this background, it will be required to suppress the EMI generated by power converters over a wide range of bandwidth from several kHz to 100 MHz or more in the near future.

Furthermore, ensuring a stable supply of electrical energy and building and utilizing advanced information and communication networks are stipulated as important. To achieve these, practical application of smart grids and microgrids that control energy transfer by fusing power conversion technology, and communication network technology and full-scale introduction of 5G communication technology are expected. Against this background, the number of cases where information and communication devices are placed near power converters is increasing, and it is necessary to discuss how to ensure electromagnetic compatibility that considers mutual interference between the power converters and the information communication devices, which is different from the EMI generation mechanism that targets only conventional power conversion systems [(19)].

The purpose of this paper is to provide a review of the advances in EMI modeling and suppression techniques and to provide future prospects in this field. The structure of this paper is as follows. First, in Chapter 2, the effect of

Invited Review Paper

a) Correspondence to: Shotaro Takahashi. E-mail: s.takahashi@st.seikei.ac.jp
[*] Department of Systems Design Engineering, Faculty of Science and Technology, Seikei University
3-1-1, Kichijoji, Kitamachi, Musashino, Tokyo 180-8633, Japan
[**] Graduate School of Systems Design, Tokyo Metropolitan University
1-1, Minami-osawa, Hachioji, Tokyo 192-0397, Japan
[***] National Institute of Technology, Tokyo College
1220-2, Kunugida-Machi, Hachioji, Tokyo 193-0997, Japan
[****] Faculty of Information Science and Technology, Hokkaido University
Kita 14, Nishi 9, Kita-Ku, Sapporo, Hokkaido 060-0814, Japan

the switching speed of power semiconductor devices on the frequency spectrum of the switching waveform of the power converter is shown. Chapter 3 presents a review of EMI modeling techniques. Chapter 4 provides a comprehensive review of EMI suppression techniques. Chapter 5 summarizes this paper, and Chapter 6 presents future prospects based on the technological trends related to EMI shown in this paper.

2. Frequency Spectra of Switching Waveforms

In general, a power converter outputs a square wave voltage of cycle T based on the switching operation of a power semiconductor device. Since the actual power semiconductor device has a voltage rise time τ_r and voltage fall time τ_f, the output voltage waveform of the power converter is a trapezoidal wave as shown in Fig. 1. The amplitude of the nth harmonic component obtained by expanding the Fourier series of the waveform in Fig. 1 can be expressed by the following equation (1) [20].

$$|A(n)| = 2A\frac{\tau}{T}\left|\frac{\sin(n\pi\tau/T)}{n\pi\tau/T}\right|\left|\frac{\sin(n\pi\tau_r/T)}{n\pi\tau_r/T}\right| \quad (1)$$

Where, the duty cycle is 0.5 and $\tau_r = \tau_f$. In the above equation, if $n = fT$, the following equation (2) which expresses equation (1) with respect to frequency f, is obtained.

$$|A(f)| = 2A\frac{\tau}{T}\left|\frac{\sin(\pi\tau f)}{\pi\tau f}\right|\left|\frac{\sin(\pi\tau_r f)}{\pi\tau_r f}\right| \quad (2)$$

Where, the envelope is defined as the following equation (3) [20].

$$\text{envelope of } \left|\frac{\sin x}{x}\right| = \begin{cases} 1 & (x < 1) \\ \dfrac{1}{|x|} & (x \geq 1) \end{cases} \quad (3)$$

Therefore, the envelope of the harmonic component can be expressed by the following equation (4).

$$\text{envelope of } |A(f)| = \begin{cases} 2A\dfrac{\tau}{T}\cdot\dfrac{1}{\pi\tau f} & \left(\dfrac{1}{\pi\tau} \leq f < \dfrac{1}{\pi\tau_r}\right) \\ 2A\dfrac{\tau}{T}\cdot\dfrac{1}{\pi\tau f}\cdot\dfrac{1}{\pi\tau_r f} & \left(\dfrac{1}{\pi\tau_r} \leq 1\right) \end{cases} \quad (4)$$

Table 1 shows the typical switching speeds of Si-IGBT, which is a power semiconductor device widely used in the past, and SiC-MOSFET and GaN-Transistor, which are WBG power semiconductor devices. Table 1 shows the switching frequency ($f_{sw} = 1/T$) when the calculation is performed for each device. Figure 2 shows a comparison of the envelopes of the Fourier series expansion of the switching voltage waveform for each device based on the switching speed shown in the table and equation (4). Here, the amplitude A of the trapezoidal wave is set to 200 V.

As shown in Fig. 2, the frequency spectra of the trapezoidal wave decrease at a slope of −20 dB/dec from the switching frequency, and at a slope of −40 dB/dec in the high frequency range due to the rise time. That is, even if the rise time τ_r is equal, each frequency component increases ten times when the switching frequency is set ten times. The WBG power semiconductor devices can switch ten times faster than Si-IGBT. Hence, by adopting WBG power semiconductor devices, the switching loss can be dramatically reduced, and by

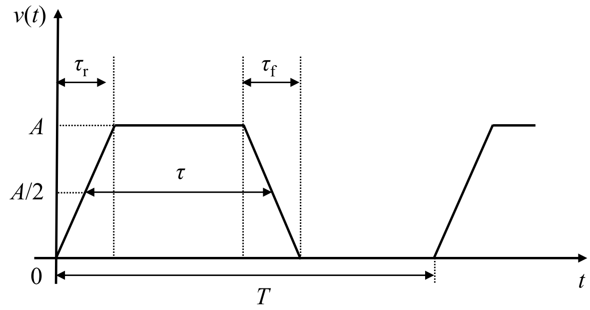

Fig. 1. Switching waveform

Table 1. Specification of power devices

	f_{sw}	τ_r
Si-IGBT	10 kHz	0.4 µs
SiC-MOSFET	100 kHz	0.03 µs
GaN-Transistor	1 MHz	0.005 µs

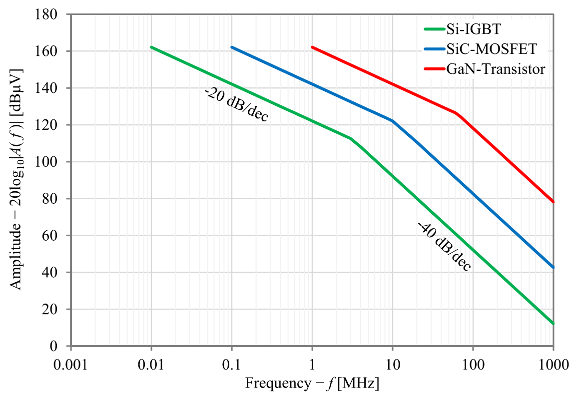

Fig. 2. Envelopes of frequency spectra of switching waveforms

increasing the switching frequency of the power converter, the size of the passive component can be reduced. However, from Fig. 2, it can be seen that the output voltage amplitudes, which was largely attenuated in the higher frequencies than 10 MHz in Si-IGBT, increase more than ten times in the frequencies of several tens of MHz.

Here, the conducted EMI is generally measured as the voltage V_N applied to the resistance sensing of the line impedance stabilization network (LISN) located on the power supply side of the power converter. V_N can be expressed by the following equation (5) based on the voltage V_{conv} output by the power converter and the transmission characteristic G_{v-v} of the noise propagation path.

$$V_N = G_{v-v} \cdot V_{conv} \quad (5)$$

As shown previously, the use of the WBG power semiconductor devices means an increase of V_{conv} in the high frequency band. In other words, with the practical use of the WBG power semiconductor devices, it is expected that the EMI generated by power converters will increase up to a band of about 1 GHz.

In order to suppress EMI, it is important to properly estimate the EMI generated by the power converter during its design stage. For this reason, various modeling methods for identifying transmission characteristic of the noise propagation path G_{v-v} have been studied until now. Moreover, as clarified by equation (5), in order to reduce EMI, either G_{v-v} should be changed or V_{conv} should be reduced. Soft switching technology and multi-level power converters can be adopted to reduce V_{conv}. G_{v-v} can be changed by adding filter components such as inductors and capacitors. This paper presents a review of EMI modeling methods in the next chapter, and Chapter 4 presents a review of EMI filtering techniques.

3. EMI Modeling Methods

As mentioned earlier, conducted EMI is measured as the voltage applied across the sensing resistance of LISN (50 Ω) located on the power supply side of the power converter. Conducted EMI has regulated values in the frequency band of 150 kHz to 30 MHz in CISPR, etc., and all power converters must meet the regulated values. Therefore, it is essential to understand the noise generation mechanism and the required noise attenuation in the design stage of the power converter.

Circuit simulators have been used for the above purposes, and many modeling methods have been proposed. In this chapter, we describe time-domain modeling and frequency domain modeling, which are typical modeling methods, as well as behavioral modeling, which is an advanced form of frequency domain modeling.

3.1 Time-domain Modeling In time-domain modeling, the entire power conversion system including LISN and load is built on the circuit simulator and then the simulation is executed. The frequency spectrum of the noise terminal voltage is obtained by conducting frequency analysis on the time-domain waveform of the acquired noise terminal voltage [(21)–(32)]. In this modeling method, it is necessary to understand the stray impedances of all the components of the system. For that reason, broadband models of passive components [(33)–(37)], power cables [(38)–(46)] and motors [(47)–(51)], electromagnetic analysis of stray components generated in circuit layouts [(31)(32)(52)] and detailed simulation models of power semiconductor devices [(52)–(60)], etc. are being investigated.

By modeling each component in detail, the simulation accuracy is improved, but the calculation time of the simulation is increased. Hence, in many cases, the power semiconductor devices are replaced with ideal components or trapezoidal wave voltage sources which simulate *dv/dt* of the power devices are implemented as noise sources. These simplifications greatly reduce the execution time of the simulation, however, the accuracy of the model in the high frequency range deteriorates. Furthermore, in time-domain modeling, it is necessary to simulate the impedance inside the power converter in detail to enhance the accuracy of the model, but it is not easy to obtain from off-the-shelf power converters.

3.2 Frequency-domain Modeling To overcome the above issues in time-domain modeling techniques, frequency-domain modeling methods have been investigated [(61)–(67)]. In frequency-domain modeling, the frequency spectrum of conducted EMI is acquired by multiplying the frequency spectrum of the noise source by the frequency characteristics of the noise propagation path. These modeling methods can significantly reduce the simulation time compared to time-domain modeling methods. In frequency domain modeling, modeling is often focused on either the differential mode (DM) or common mode (CM) of the target power conversion system. The frequency spectrum of the total conducted EMI is obtained by adding the results obtained from the model for each mode.

However, even in frequency domain modeling, the simulation accuracy depends on the modeling accuracy of each component of the power conversion system. In addition, although the simulation accuracy can be improved by using the measured switching waveforms of the power semiconductor device as a noise source, switching waveforms are not easily available for all power converters.

3.3 Behavioral Modeling Behavioral modeling is a modeling method investigated for the purpose of further improving the accuracy of frequency domain modeling [(68)–(80)]. Behavioral modeling is described below using the conducted EMI measurement setup based on the DC fed buck converter shown in Fig. 3 as an example. The buck converter is constructed using SiC-MOSFETs (SCT3020AL, Rohm) and is operated with the following conditions: input DC voltage 200 V, switching frequency 100 kHz, duty 0.5, and output power 100 W. For the setup shown in Fig. 3, a behavioral model can be derived as shown in Fig. 4 using the CM noise voltage source V_{CM}, DM noise current source I_{DM}, CM noise propagation path impedance Z_{CM}, and DM noise propagation path impedance Z_{DM} [(78)]. In Fig. 4, Z_{LISN} is the impedance of DC-LISN. These impedances are measured using an impedance analyzer or vector network analyzer, and an equivalent circuit is constructed on the circuit simulator. The equivalent noise source V_{CM} and I_{CM} can be calculated from the measured DC bus currents I_P and I_N through equations (6) and (7) below [(78)].

$$V_{CM} = (I_P + I_N) \cdot \left(\frac{Z_{LISN}}{2} + Z_{CM} \right) \cdots\cdots\cdots\cdots\cdots\cdots (6)$$

$$I_{DM} = (I_P - I_N) \cdot \left(\frac{Z_{LISN}}{4Z_{CM}} + \frac{Z_{LISN}}{Z_{DM}} + \frac{1}{2} \right) \cdots\cdots\cdots\cdots (7)$$

Here, assuming that the voltages appearing at the measured terminals of each DC-LISN are $V_{LISN,P}$ and $V_{LISN,N}$, the CM components $V_{N,CM}$ of the conducted EMI in this system can

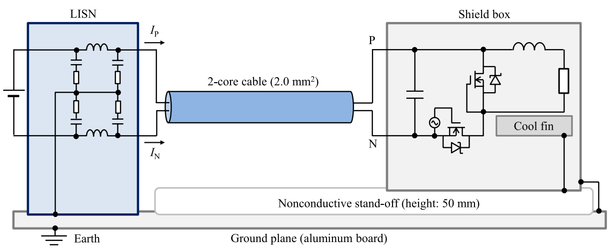

Fig. 3. Experimental setup for measurement of conducted EMI

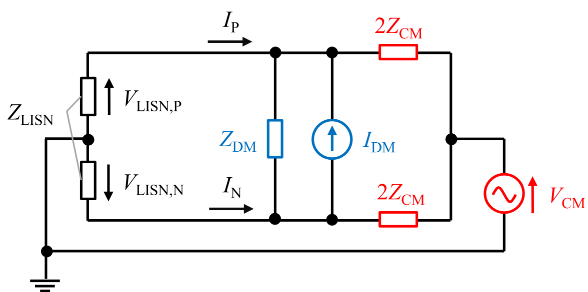

Fig. 4. Generalized behavioral EMI model according to (78)

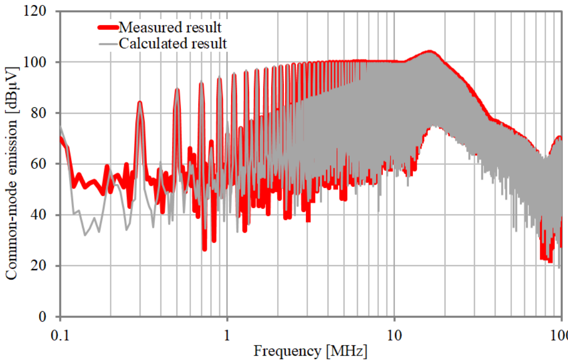

Fig. 5. Comparison between measured and calculated CM component of conducted EMI

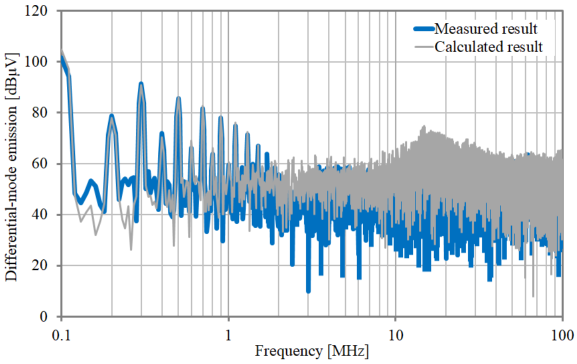

Fig. 6. Comparison between measured and calculated DM component of conducted EMI

be expressed by the following equation (8).

$$V_{\mathrm{N,CM}} = \frac{V_{\mathrm{LISN,P}} + V_{\mathrm{LISN,N}}}{2} \quad \cdots\cdots (8)$$

In addition, if the transfer function $G_{\mathrm{v-v,CM}}$ from CM noise voltage source V_{CM} to the measured voltage across the sensing resistance of LISN are obtained using circuit simulator, the CM component of the conducted EMI can be calculated from equation (9) below.

$$V_{\mathrm{N,CM,cal}} = G_{\mathrm{v-v,CM}} \cdot V_{\mathrm{CM}} \quad \cdots\cdots (9)$$

Figure 5 shows a comparison between the measured results and the calculated results of the CM component of conducted EMI in the system in Fig. 3. From Fig. 5, it is clear that the model reproduces the CM component of the conducted EMI over a wide band from 100 kHz to 100 MHz.

Next, the DM components $V_{\mathrm{N,DM}}$ of conducted EMI can be expressed by equation (10) below.

$$V_{\mathrm{N,DM}} = \frac{V_{\mathrm{LISN,P}} - V_{\mathrm{LISN,N}}}{2} \quad \cdots\cdots (10)$$

In addition, when the transfer functions $G_{\mathrm{i-v,DM}}$ from the DM noise current source I_{DM} to the measured voltage across the sensing resistance of LISN are obtained using the circuit simulator, the DM component of conducted EMI can be calculated from the equation (11) below.

$$V_{\mathrm{N,DM,cal}} = G_{\mathrm{i-v,CM}} \cdot I_{\mathrm{DM}} \quad \cdots\cdots (11)$$

Figure 6 shows a comparison between the measured results and the calculated results of the DM component of the conducted EMI. It can be seen that the model also reproduces the DM component over a wide band. It is also clear from Figs. 5 and 6 that the DM noise is dominant in 1 MHz band or less, and the CM noise is dominant in 1 MHz band or over in this system.

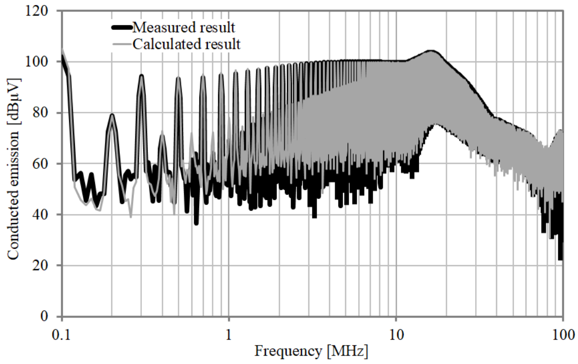

Fig. 7. Comparison between measured and calculated conducted EMI

Figure 7 shows a comparison between the measured results and the calculated results of the conducted EMI. The conducted EMI was obtained as the sum of the calculation results of the CM and DM components of the measured terminal voltage of the LISN. It is clear from Fig. 7 that the constructed model can reproduce the conducted EMI generated by the system over a wide band from 100 kHz to 100 MHz.

Behavioral modeling is useful in the design of EMI filters because of the extremely short simulation calculation time and high accuracy over a wide band. On the other hand, since the power converter and noise propagation path are completely black-boxed, it becomes difficult to understand the noise generation mechanism from the constructed model.

4. EMI Filtering Techniques

In this chapter, we review the techniques for suppressing conducted EMI. Conducted EMI suppression techniques are broadly divided into the use of EMI filters, changes in circuit topologies, and improvements in modulation methods. This paper focuses on techniques that use EMI filters. The EMI filters can be classified into passive EMI filters consisting of only passive components, and active EMI filters that use active components such as complimentary transistors and/or operational amplifiers.

4.1 Passive EMI Filters

4.1.1 Line-side Filtering Figure 8 shows the EMI filter with the most common configuration using passive components. The EMI filter consists of a common mode inductor (CMI), Y capacitors, which are CM noise filtering components, differential-mode inductors (DMIs) and X capacitors, which are DM noise filtering components. The CMI is realized by applying windings with the same polarity to a magnetic core. The leakage inductance of CMI is often used as the DMI to reduce the number of filter components. The most basic EMI filter design procedure is presented in Ref. (81). EMI filters are typically installed on the input side of the power converter, where the inductor increases the impedance of the noise propagation path, and the capacitor provides a low impedance bypass path to the noise current, greatly reducing the conducted EMI.

On the other hand, it has been pointed out that the EMI

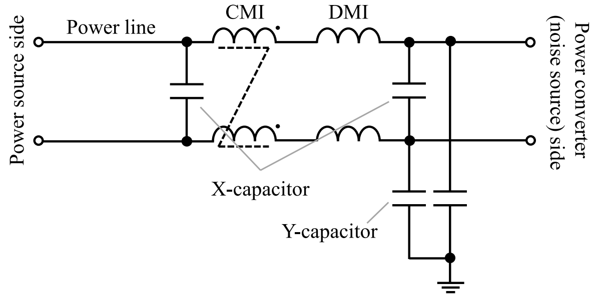

Fig. 8. Basic structure of an EMI filter

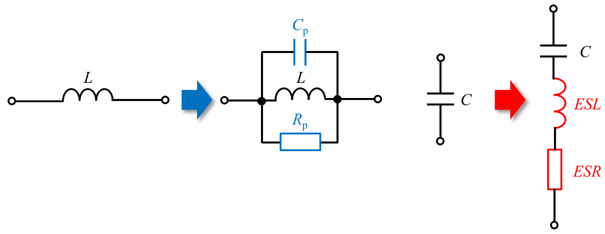

Fig. 9. Equivalent circuits of filter components

filter occupies about 30% of the volume of the entire power converter [(82)–(84)]. Therefore, design methods for EMI filters that obtains the minimum volume has been widely studied [(85)–(87)]. In particular, the volume ratio of CMI in entire EMI filter is large. Hence, design methods that consider the magnetic saturation of CMI have been proposed [(88)(89)]. Furthermore, in Refs. (90)–(94), an attempt is made to reduce the filter volume by using a planar inductor with a printed circuit board pattern as the windings.

As shown in Fig. 9, stray impedances of passive components strongly influence on the frequency characteristics of the filtering components. Since the inductor has a stray capacitance (C_p) and iron loss resistance (R_p), the impedance of the actual inductor can be represented as these parallel connection circuits. In capacitors, there are also stray impedances generally known as an equivalent series inductance (*ESL*) and an equivalent series resistance (*ESR*). If these stray impedance components are considered, the impedance of a real capacitor is represented as a series connection circuit of the capacitance *C*, *ESL*, and *ESR*. In general, the impedance of an ideal inductor without a stray impedance increases with a slope of +20 dB/dec (inductive impedance), and the impedance of an ideal capacitor decreases with a slope of −20 dB/dec (capacitive impedance). However, in a real passive element in which stray impedances exist, self-resonance occurs, and at frequencies after that, the inductor behaves as a capacitive impedance and the capacitor behaves as an inductive impedance.

The stray impedance also has a great influence on the attenuation of the EMI filter. In general, the performance of EMI filters is evaluated with insertion loss obtained from the measurement system which is terminated at 50 Ω. As an example, the insertion loss of the LC low-pass filter is shown in Fig. 10. First, when a filter is manufactured using only ideal elements, it shows an attenuation characteristic of −40 dB/dec from the cutoff frequency (dotted line in Fig. 10). On the other hand, if the stray impedance of each filter component is considered, the attenuation in the high-frequency range changes

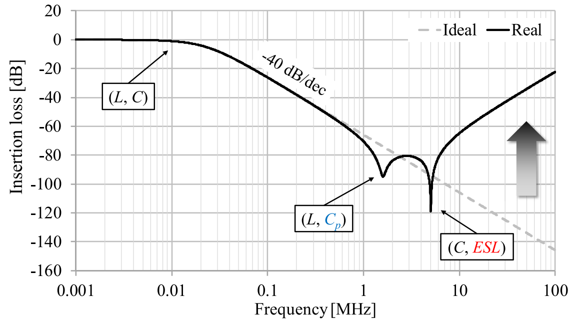

Fig. 10. Calculated insertion loss of the EMI filter with stray impedance components (L = 1 mH, C_p = 10 pF, R_p = 100 kΩ, C = 100 nF, ESL = 10 nH, ESR = 1 mΩ)

significantly. From the cutoff frequency of the LC low-pass filter to a certain frequency, an attenuation characteristic of −40 dB/dec is shown, but at around 1 MHz, the filter inductor occurs a self-resonance due to the stray capacitance C_p, and the filter attenuation stops dropping at about −80 dB. In addition, the fact that the filter capacitor causes self-resonance with *ESL* near 5 MHz can be confirmed. Hence, the attenuation of the EMI filter continues to deteriorate in the high frequency range of 5 MHz or higher. In other words, it is important to reduce the stray impedance in order to realize an EMI filter that has a large attenuation in the high frequency range.

In general, the frequency characteristics of almost all capacitors can be simulated by the equivalent circuit shown in Fig. 9. In addition, the stray impedance of the capacitor is a parameter that is difficult to change by designers of EMI filters. On the other hand, inductors are more complicated components whose frequency characteristics change depending on multiple factors such as the frequency dependence of the complex permeability of magnetic materials and winding resistance. The stray impedance of inductors can be controlled by the filter designer by selecting the magnetic material and changing the winding arrangement. That is, the fact that the impedance of the inductor can be estimated according to the selected magnetic material and the winding arrangement applied to the magnetic core in the design stage is useful to achieve an EMI filter that has a large amount of attenuation over a wide band. To realize this, analysis models [(95)–(98)] and circuit simulation models [(99)–(104)] for simulating the frequency characteristics of inductors, as well as stray capacitance estimation methods [(105)–(112)], etc. are being investigated.

It has also been pointed out that an inter-parasitic coupling between the filtering components is also a factor that deteriorates the attenuation of the EMI filter in the high frequency range [(113)–(115)]. Attempts have also been made to reproduce inter-parasitic coupling inside the EMI filter by performing three-dimensional electromagnetic field analysis [(116)(117)].

4.1.2 Load-side Filtering In motor drive systems, CM current i_{cm} flows through the motor stray capacitance, thus, noise filtering techniques are often taken not only on the input side of the power converter but also on the output side in order to suppress the shaft voltage and bearing current of the motor, as well as the radiated noise from the power cable. Here, filtering techniques for suppressing the output side noise are described taking the three-phase inverter fed motor

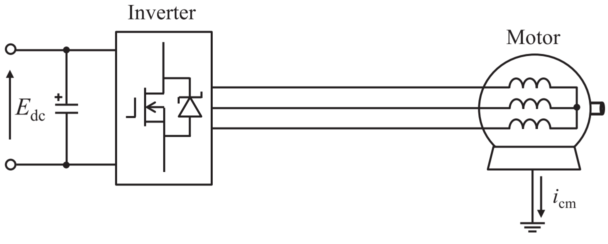

Fig. 11. Three-phase PWM inverter fed motor drive system

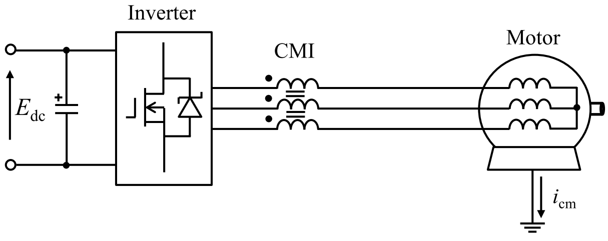

Fig. 12. Common-mode inductor installed at the output-side of the motor drive system

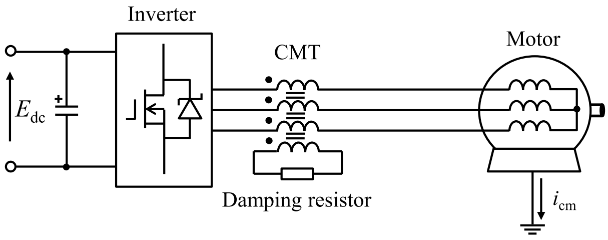

Fig. 13. Common-mode transformer for damping the resonance of the output-side common-mode current

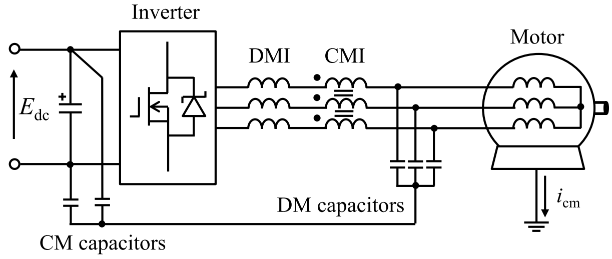

Fig. 14. Output-side LC filter with DC feedback

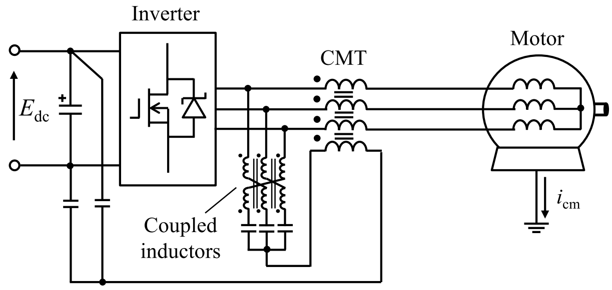

Fig. 15. Passive canceller based on coupled inductors and a common-mode transformer

drive system shown in Fig. 11 as an example.

The simplest noise filtering technique on the output side is installing CMI [118]–[120]. In this technique, as shown in Fig. 12, a three-phase CMI is installed on the output side of the motor drive system and the CMI current i_{cm} is suppressed by increasing the CM impedance. However, in many cases, the CMI with a very large CM inductance is required to sufficiently suppress the CM current. Hence, the turn numbers of the CMI increases, resulting in an increase in winding stray capacitance. By using magnetic materials with high relative permeability such as nanocrystalline as the magnetic core material of CMI, the decrease of the turns can be expected. However, the relative permeability of these magnetic materials decreases from several tens of kHz [28][120]–[122]. For this reason, the volume of CMIs fabricated under the condition that the switching frequency of the motor drive system is set to about 200 kHz is larger than that of the CMI fabricated under the condition that the switching frequency of the drive is set to 20 kHz [122]. In addition, as shown in Fig. 13, a technique for damping the resonance of the CM current by short-circuiting with resistance the secondary winding of a common-mode transformer (CMT) which is realized by adding a secondary winding to the three-phase CMI has also been proposed [7]. This technique is effective in suppressing the peak value of CM current, but it cannot reduce the rms value. Furthermore, an increase in loss due to the addition of damping resistance can also be a problem.

By using an LC CM filter consists of CMI and Y capacitors with feedback neutral point of capacitors to DC link, the volume of the core of the three-phase CMI needs only have a size that does not saturate against the CM voltage output by the inverter [123][124]. Hence, compared to the method of inserting only the three-phase CMI, volume miniaturization can be expected. However, in using a Y capacitor, short-circuit is necessary at the output of the inverter with a capacitor. Because of this, a large current may flow between the phases of the inverter. To prevent this, a DMI must be inserted in each inverter output phase, as shown in Fig. 14. Normally, the size of the DMI is increased such that its design does not saturate against the load current of the motor drive system. Also, if the percentage impedance of the DMI is large compared to the motor inductance, most of the inverter output voltage will be applied to the DMI. In order to solve the above problem, a method has been proposed to draw out the neutral point of the three-phase motor and feed it back to the DC bus [125]. In this method, although it is necessary to change the structure of the motor, the advantage is that the large DMI can be omitted by actively using the motor inductance [125]–[129]. There have been detailed reports regarding this method, such as the suppression effect towards the leaked current from the heat sink [128], and the suppression effect towards the bearing current [127].

Figure 15 shows the measures against CM noise on the output side of a motor drive system that uses a passive canceller [130]. This method is characterized by the sensing of the CM voltage generated by the inverter using three coupled inductors. An ideal coupled inductor has a large impedance towards the DM component and no impedance towards the CM component. Hence, by using coupled inductors, the CM voltage can be sensed by a relatively large Y capacitor. By applying the sensed CM voltage to the CMT with a winding ratio of 1 : 1, the CM voltage output by the inverter can be cancelled. In addition, techniques such as combining a passive canceller with an LC filter [131], or with an active feedback circuit [132] have been proposed.

4.2 Active EMI Filters Active EMI filters that use

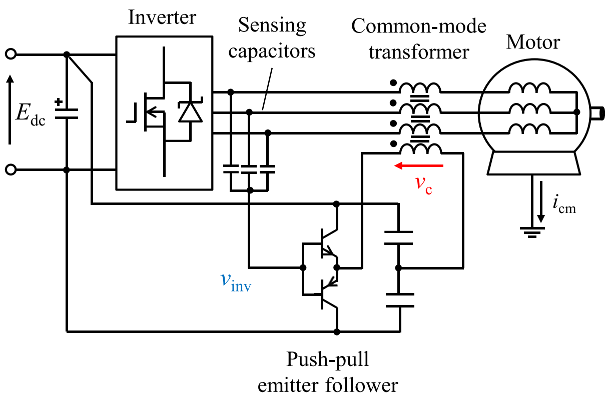

Fig. 16. Feedforward voltage compensation type active EMI filter

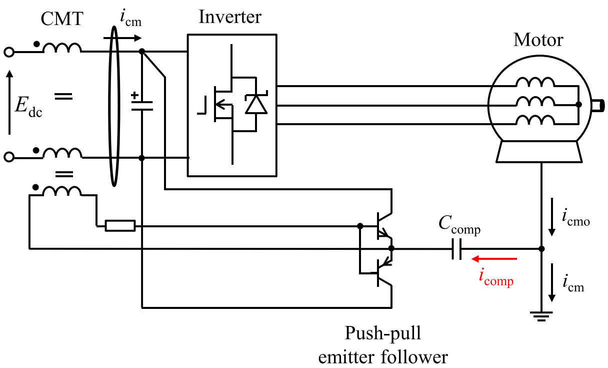

Fig. 17. Feedforward current compensation type active EMI filter

active components have been proposed in order to improve the attenuation characteristic of passive EMI filters and significantly reduce their size and weight [133–152]. Active EMI filters are roughly classified into the feedforward method [133–141] and feedback method [142–152].

Feedforward active EMI filter is roughly classified into two types: voltage compensation method [133–135] and current compensation method [136–141]. Active common noise canceller (ACC) has been proposed as a typical example of a feedforward voltage compensation active EMI filter [133]. As shown in Fig. 16, the ACC senses the CM voltage output by the three-phase PWM inverter and cancels the CM voltage by applying a reverse phase voltage to the CMT via a buffer composed of a push-pull emitter follower. It has been proven that the ACC can almost completely suppress the CM current on the output side in a motor drive system. On the other hand, one issue with this is that the applications to which the ACC can be applied are limited due to the withstand voltage of complementary transistors. Hence, there is a study aimed at increasing the withstand voltage of ACC [134]. Also, in order to improve the deterioration of the CM voltage suppression performance that arises from the crossover distortion of the push-pull emitter follower, a method using an active feedback circuit in combination has also been proposed [135].

Figure 17 shows the typical configuration example of the feedforward current compensation type active EMI filter [136]. In this method, a bypass path for the compensation current i_{comp} is provided by the push-pull emitter follower so that the CM current i_{cm} sensed using the CMT becomes zero. This method also limits the applications that can be applied

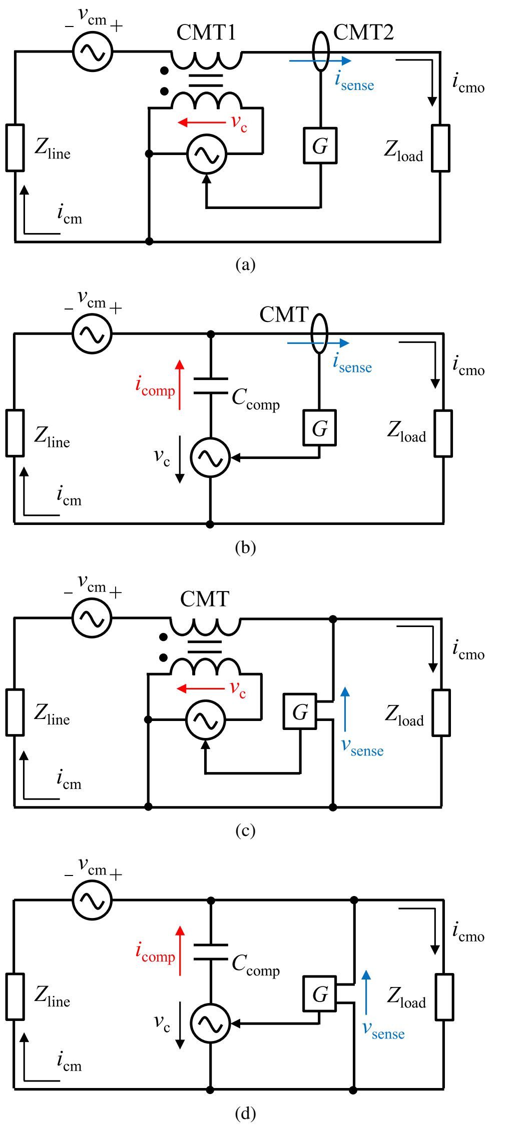

Fig. 18. Basic structure of feedback type active EMI filters. (a) Current-sensing series-compensation (CSSC) type. (b) Current-sensing parallel-compensation (CSPC) type. (c) Voltage-sensing series-compensation (VSSC) type. (d) Voltage-sensing parallel-compensation (VSPC) type

depending on the withstand voltage of the complementary transistor. Hence, several approaches to achieve high withstand voltage have been proposed [137][138][140].

The feedback method can be classified into the four types shown in Fig. 18 based on the noise sensing method and compensation method [152]. First, in the current sensing series compensation (CSSC) method [142][143], shown in Fig. 18(a), the noise current is sensed using CMT2, and the feedback compensation voltage v_c is inserted in series towards the noise voltage source v_{cm} via CMT1. The feedback compensation voltage source is realized by a high-speed operational amplifier. A merit of the CSSC method is that the feedback compensation voltage source can be electrically insulated from the power conversion circuit using two CMTs. In the current sensing parallel compensation (CSPC) method [144][145] shown in Fig. 18(b), the feedback compensation voltage source is inserted in parallel towards the noise voltage source using

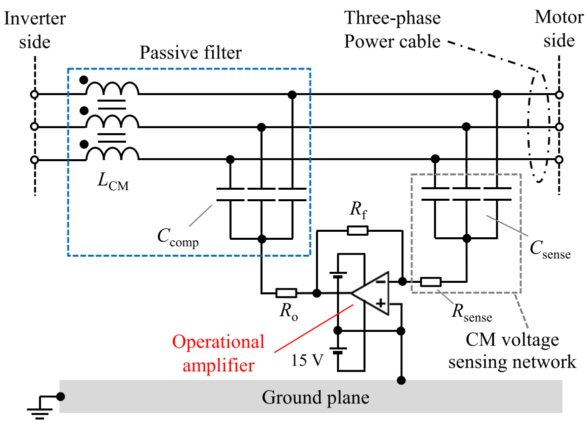

Fig. 19. The structure of the ACF installed at the output-side of the three-phase motor drive system

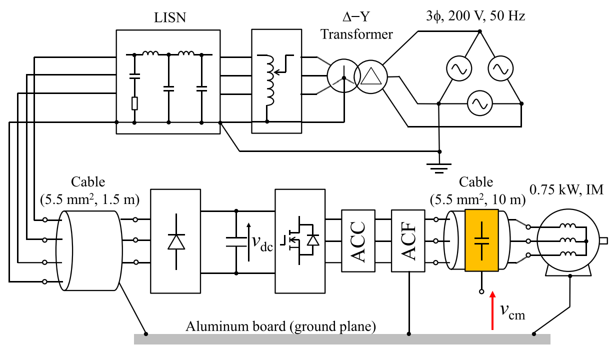

Fig. 20. Experimental setup for measurement of CM voltage

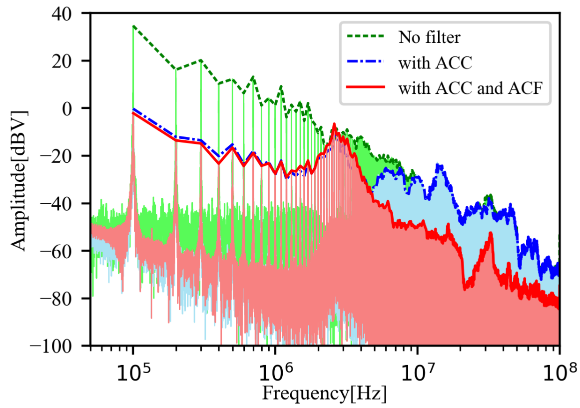

Fig. 21. Frequency analysis results of the measured CM voltage waveforms

compensation capacitor C_{comp}. In the voltage sensing series compensation (VSSC) method (146)–(148), shown in Fig. 18(c), the noise voltage is the sensing target, and the feedback compensation voltage source is inserted in series towards the noise voltage source via the CMT. In the voltage sensing parallel compensation (VSPC) method (149)–(152) shown in Fig. 18(d), the noise voltage is sensed, and the feedback compensation voltage v_c multiplied by G is inserted in parallel towards the noise voltage source via the compensation capacitor. Unlike the other three methods, the VSPC method does not require an additional CMT to sense and compensate for noise signals. In general, it is difficult to realize a CMT with a wide operating frequency range due to the frequency dependence of the complex permeability of the magnetic material and the winding stray capacitance. Therefore, the VSPC method, which does not require CMT, is a feedback method active EMI filter suitable for high frequency application.

In Ref. (150), active common-mode filter (ACF) which is a VSPC active EMI filter, has been proposed. Figure 19 shows the configuration of the ACF placed on the output side of the three-phase motor drive system. The three-phase CMI L_{CM} and the compensation capacitor C_{comp} make up the LC filter. The CM voltage output by the PWM inverter is sensed by a high-pass filter circuit composed of C_{sense} and R_{sense}. The sensed CM voltage is feedbacked to the compensation capacitor with an inverting amplifier circuit with a gain of G times realized through a high-speed operational amplifier. This feedback compensation increases the capacitance of the compensation capacitor by $1 + G$ times in the high frequency range. As a result, the cutoff frequency of the LC filter shifts to the low frequency range. That is, the attenuation of the LC filter can be increased in the high frequency range without increasing the size of the filtering component.

In Ref. (152), a wideband CM voltage suppression method by using ACC and ACF together is studied for three-phase motor drive systems. Figure 20 shows the configuration of the experimental setup in Ref. (152). The CM voltage v_{cm} is measured as the voltage between the shield applied to the cable (realized by wrapping a copper tape around the three-phase power cable) and the ground plane. The CM voltage was measured under the conditions that the switching frequency of the PWM inverter was set to 100 kHz, the output frequency was set to 50 Hz, and the DC link voltage was set to 200 V. Figure 21 shows the frequency analysis results for the measured CM voltage. It is clear from Fig. 21 that by applying ACC, the CM voltage generated by the inverter can be suppressed from a fundamental frequency band of 100 kHz to about 7 MHz. However, due to the frequency characteristic of the CMT, the attenuation of the ACC with respect to the CM voltage deteriorates from about 1 MHz. On the other hand, the ACF attenuates the CM voltage by about 20 dB from about 4 to 100 MHz. In other words, by using the ACC and the ACF together, the CM voltage generated by the three-phase PWM inverter fed motor drive system can be significantly suppressed over wide band frequencies from 100 kHz to 100 MHz.

5. Summary

This paper reviewed the evolution of modeling and suppression techniques for EMI in power conversion systems.

First, Chapter 2 presented the effect of the switching speed of WBG power semiconductor devices such as SiC-MOSFETs and GaN-transistors on the frequency spectrum of the switching waveform of power converters. Analysis results showed that, by adopting the WBG power devices, the output voltage amplitude, which was significantly attenuated in 10 MHz or over band in conventional Si-IGBT, increases 10 times or over in more than several tens of MHz. Hence, along with the practical application of the WBG power semiconductor devices, the EMI generated by power converters will increase to a band of about 1 GHz. In other words, EMI countermeasures become even more important in power converter designs.

Chapter 3 presented a review of the EMI modeling methods. The three methods, namely, time-domain modeling, frequency-domain modeling, and behavioral modeling were outlined. The usefulness of the DC fed buck converter was presented as an example of behavior modeling.

Chapter 4 presented a comprehensive review of EMI suppression techniques in power converters. The suppression technique that used the most widely adopted EMI filter was described in this paper. EMI filters are broadly classified into the passive EMI filters which used passive components, and active EMI filter which used active components. First, the basic configuration of the passive EMI filter was shown, then it was stated that the high frequency characteristics of the filter deteriorate due to stray impedance, and that volume minimization design has been actively studied. The filtering techniques that suppress the output side noise of the motor drive system was also summarized. Next, it was stated that active EMI filters can be broadly divided into the feedforward and feedback methods. In addition, it was also shown that the feedback method can be classified into four types according to the noise sensing and compensating method. Taking a three-phase inverter fed motor drive system as an example, it was shown that by combining a feedforward active EMI filter (ACC) and a feedback active EMI filter (ACF), the CM voltage output by the three-phase inverter can be suppressed by about 20 dB over wide band frequencies from 100 kHz to 100 MHz.

6. Future Perspective

Important future research topics related to EMI in power conversion systems are described below.

- Simulation model: In many simulation models, the effect of electromagnetic coupling between the components that make up the power converter on EMI is not considered. Hence, in many models, the simulation accuracy deteriorates in 10 MHz or over high frequency band. It is necessary to improve the simulation accuracy by realizing a model that considers parasitic coupling. In addition, it is important to establish a power converter design method that optimizes component placement from the perspective of EMI reduction based on the model.
- Passive EMI filter: Further research is needed on the thermal model of filtering components, circuit simulation model that considers the mutual coupling between filtering components, and optimum design that considers the stray impedance of filtering components.
- Active EMI filter: The problem with active EMI filters is that the reliability of the entire system is reduced when active components are adopted. In particular, a detailed evaluation of the stability, loss, and power supply of active EMI filters is needed.
- Conducted EMI for a frequency range below 150 kHz: DM noise becomes dominant in the low frequency band of several tens of kHz. Hence, a very large EMI filter is required to suppress EMI in this band. To reduce the filter size, it is necessary to study an active EMI filter that can reduce EMI in the low frequency band of 150 kHz or lower.
- Radiated EMI: With power converters turning to high-frequency drive, the radiated EMI that they generate in several tens of MHz band or higher will increase significantly. Therefore, it is necessary to study the radiated EMI generation mechanism, the analysis model of radiated EMI based on the generation mechanism, and effective radiated EMI suppression methods.
- EMI for multiple power converter systems: The EMI generation mechanism at the system level such as distribution networks (systems that consist of multiple power converters and loads such as microgrids) should be investigated and modeling methods must be established.
- Mutual interference between power converters and information communication equipments: With the recent practical application of smart grids and microgrids and the introduction of 5G communication technology, many information communication devices are being placed near power converters. For this reason, it is necessary to discuss how to ensure electromagnetic compatibility with respect to mutual interference between the power converters and the information communication devices, which is different from the EMI generation mechanism that targeted only conventional power conversion systems.

References

(1) R. Redl: "Power electronics and electromagnetic compatibility", *PESC Record. 27th Annual IEEE Power Electronics Specialists Conference*, Vol.1, pp.15–21 (1996)

(2) G.L. Skibinski, R.J. Kerkman, and D. Schlegel: "EMI emissions of modern PWM AC drives", *IEEE Industry Applications Magazine*, Vol.5, No.6, pp.47–80 (1999)

(3) M.J. Nave: "Power line filter design for switched mode power supplies", 2nd Edition. Mark Nave Consultants (2010)

(4) D. Boroyevich, X. Zhang, H. Bishinoi, R. Burgos, P. Mattavelli, and F. Wang: "Conducted EMI and systems integration", *CIPS 2014; 8th International Conference on Integrated Power Electronics Systems*, pp.1–12 (2014)

(5) Y. Murai, T. Kubota, and Y. Kawase: "Leakage current reduction for a high-frequency carrier inverter feeding an induction motor", *IEEE Trans. on Industry Applications*, Vol.28, No.4, pp.858–863 (1992)

(6) E. Zhong and T.A. Lipo: "Improvements in EMC performance of inverter-fed motor drives", *IEEE Trans. on Industry Applications*, Vol.31, No.6, pp.1247–1256 (1995)

(7) S. Ogasawara and H. Akagi: "Modeling and damping of high-frequency leakage currents in PWM inverter-fed AC motor drive systems", *IEEE Trans. on Industry Applications*, Vol.32, No.5, pp.1105–1114 (1996)

(8) D.M. Hockanson, J.L. Drewniak, T.H. Hubing, T.P. Van Doren, F. Sha, and M.J. Wilhelm: "Investigation of fundamental EMI source mechanisms driving common-mode radiation from printed circuit boards with attached cables", *IEEE Trans. on Electromagnetic Compatibility*, Vol.38, No.4, pp.557–566 (1996)

(9) S. Chen, T.A. Lipo, and D. Fitzgerald: "Modeling of motor bearing currents in PWM inverter drives", *IEEE Trans. on Industry Applications*, Vol.32, No.6, pp.1365–1370 (1996)

(10) S. Ogasawara, H. Ayano, and H. Akagi: "Measurement and reduction of EMI radiated by a PWM inverter-fed AC motor drive system", *IEEE Trans. on Industry Applications*, Vol.33, No.4, pp.1019–1026 (1997)

(11) J. Biela, M. Schweizer, S. Waffler, and J.W. Kolar: "SiC versus Si—evaluation of potentials for performance improvement of inverter and DC–DC converter systems by SiC power semiconductors", *IEEE Trans. on Industrial Electronics*, Vol.58, No.7, pp.2872–2882 (2011)

(12) M.M. Swamy, J.K. Kang, and K. Shirabe: "Power loss, system efficiency, and leakage current comparison between Si IGBT VFD and SiC FET VFD with various filtering options", *IEEE Trans. on Industry Applications*, Vol.51, No.5, pp.3858–3866 (2015)

(13) J.W. Kolar, D. Bortis, and D. Neumayr: "The ideal switch is not enough", *2016 28th International Symposium on Power Semiconductor Devices and*

ICs (*ISPSD*), pp.15–22 (2016)

(14) D. Bortis, D. Neumayr, and J.W. Kolar: "$\eta\rho$-pareto optimization and comparative evaluation of inverter concepts considered for the Google Little Box Challenge", *2016 IEEE 17th Workshop on Control and Modeling for Power Electronics* (*COMPEL*) (2016)

(15) L. Schrittwieser, M. Leibl, M. Haider, F. Thony, J.W. Kolar, and T.B. Soeiro: "99.3% Efficient three-phase buck-type all-SiC SWISS rectifier for DC distribution systems", *IEEE Trans. on Power Electronics*, Vol.34, No.1, pp.126–140 (2019)

(16) D. Han, S. Li, Y. Wu, W. Choi, and B. Sarlioglu: "Comparative analysis on conducted CM EMI emission of motor drives: WBG versus Si devices", *IEEE Trans. on Industrial Electronics*, Vol.64, No.10, pp.8353–8363 (2017)

(17) B. Zhang and S. Wang: "A survey of EMI research in power electronics systems with wide-bandgap semiconductor devices", *IEEE Journal of Emerging and Selected Topics in Power Electronics*, Vol.8, No.1, pp.626–643 (2020)

(18) Y. Zhang, S. Wang, and Y. Chu: "Analysis and comparison of the radiated electromagnetic interference generated by power converters with Si MOSFETs and GaN HEMTs", *IEEE Trans. on Power Electronics*, Vol.35, No.8, pp.8050–8062 (2020)

(19) R. Shirai and T. Shimizu: "Time domain analysis of transmission failure on CAN system due to differential-mode noise emitted from a buck converter", *IEEJ Journal of Industry Applications*, Vol.8, No.4, pp.608–614 (2019)

(20) C.R. Paul: "Introduction to electromagnetic compatibility", Sections 3.1 and 3.2, Wiley-Interscience (2006)

(21) L. Ran, S. Gokani, J. Clare, K.J. Bradley, and C. Christopoulos: "Conducted electromagnetic emissions in induction motor drive systems part I: time domain analysis and identification of dominant modes", *IEEE Trans. on Power Electronics*, Vol.13, No.4, pp.757–767 (1998)

(22) L. Yang, B. Lu, W. Dong, Z. Lu, M. Xu, F.C. Lee, and W.G. Odendaal: "Modeling and characterization of a 1 KW CCM PFC converter for conducted EMI prediction", *Nineteenth Annual IEEE Applied Power Electronics Conference and Exposition, 2004. APEC '04.*, pp.763–769 (2004)

(23) T. Nussbaumer, M.L. Heldwein, and J.W. Kolar: "Differential mode input filter design for a three-phase buck-type PWM rectifier based on modeling of the EMC test receiver", *IEEE Trans. on Industrial Electronics*, Vol.53, No.5, pp.1649–1661 (2006)

(24) A.C. Baisden, D. Boroyevich, and J.D. Van Wyk: "High frequency modeling of a converter with an RF-EMI filter", *Conference Record of the 2006 IEEE Industry Applications Conference Forty-First IAS Annual Meeting*, pp.2290–2295 (2006)

(25) M. Jin and M. Weiming: "Power converter EMI analysis including IGBT nonlinear switching transient model", *IEEE Trans. on Industrial Electronics*, Vol.53, No.5, pp.1577–1583 (2006)

(26) M. Moreau, N. Idir, and P. Le Moigne: "Modeling of conducted EMI in adjustable speed drives", *IEEE Trans. on Electromagnetic Compatibility*, Vol.51, No.3, pp.665–672 (2009)

(27) F. Giezendanner, J. Biela, J.W. Kolar, and S.Z. Koch: "EMI noise prediction for electronic ballasts", *IEEE Trans. on Power Electronics*, Vol.25, No.8, pp.2133–2141 (2010)

(28) M. Hartmann, H. Ertl, and J.W. Kolar: "EMI filter design for a 1 MHz, 10 kW three-phase/level PWM rectifier", *IEEE Trans. on Power Electronics*, Vol.26, No.4, pp.1192–1204 (2011)

(29) Y. Koyama, M. Tanaka, and H. Akagi: "Modeling and analysis for simulation of common-mode noises produced by an inverter-driven air conditioner", *IEEE Trans. on Industry Applications*, Vol.47, No.5, pp.2166–2174 (2011)

(30) B. Toure, J.L. Schanen, L. Gerbaud, T. Meynard, J. Roudet, and R. Ruelland: "EMC modeling of drives for aircraft applictions: modeling process, EMI filter optimization, and technological choice", *IEEE Trans. on Power Electronics*, Vol.28, No.3, pp.1145–1156 (2013)

(31) E.R. Pinilla, F. Morel, C. Vollaire, and J.L. Schanen: "Modeling of a buck converter with a SiC JFET to predict EMC conducted emissions", *IEEE Trans. on Power Electronics*, Vol.29, No.5, pp.2246–2260 (2014)

(32) M. Laour, R. Tahmi, and C. Vollaire: "Modeling and analysis of conducted and radiated emissions due to common mode current of a buck converter", *IEEE Trans. on Electromagnetic Compatibility*, Vol.59, No.4, pp.1260–1267 (2017)

(33) Q. Yu, W. Holmes, and K. Naishadham: "RF equivalent circuit modeling of ferrite-core inductors and characterization of core materials", *IEEE Trans. on Electromagnetic Compatibility*, Vol.44, No.1, pp.258–262 (2002)

(34) T. Kato, K. Inoue, and D. Kagawa: "Lumped equivalent model synthesis for a passive element with frequency-dependent and/or temperature-dependent characteristics for EMC simulation", *2009 IEEE 6th International Power Electronics and Motion Control Conference*, pp.963–969 (2009)

(35) J.L. Kotny, X. Margueron, and N. Idir: "High-frequency model of the coupled inductors used in EMI filters", *IEEE Trans. on Power Electronics*, Vol.27, No.6, pp.2805–2812 (2012)

(36) W. Tan, C. Cuellar, X. Margueron, and N. Idir: "A high frequency equivalent circuit and parameter extraction procedure for common mode choke in the EMI filter", *IEEE Trans. on Power Electronics*, Vol.28, No.3, pp.1157–1166 (2013)

(37) F. Traub, B. Wunsch, and S. Skibin: "A high frequency model of toroidal chokes for EMC filtering", *2015 IEEE International Symposium on Electromagnetic Compatibility* (*EMC*), pp.902–907 (2015)
K. Nomura, T. Kojima, and Y. Hattori: "Straightforward modeling of complex permeability for common mode chokes", *IEEJ Journal of Industry Applications*, Vol.7, No.6, pp.462–472 (2018)

(38) Y. Weens, N. Idir, J.J. Franchaud, and R. Bausiere: "High frequency model of a shielded 4-wire energy cable", *2005 European Conference on Power Electronics and Applications*, pp.1–10 (2005)

(39) Y. Weens, N. Idir, R. Bausiere, and J.J. Franchaud: "Modeling and simulation of unshielded and shielded energy cables in frequency and time domains", *IEEE Trans. on Magnetics*, Vol.42, No.7, pp.1876–1882 (2006)

(40) J. Luszcz: "Motor cable as an origin of supplementary conducted EMI emission of ASD", *2009 13th European Conference on Power Electronics and Applications*, pp.1–7 (2009)

(41) N. Idir, Y. Weens, and J.J. Franchaud: "Skin effect and dielectric loss models of power cables", *IEEE Trans. on Dielectrics and Electrical Insulation*, Vol.16, No.1, pp.147–154 (2009)

(42) J. Luszcz: "Motor cable effect on the converter fed AC motor common mode current", *2011 7th International Conference-Workshop Compatibility and Power Electronics* (*CPE*), pp.445–450 (2011)

(43) I. Stevanovic, B. Wunsch, G.L. Madonna, and S. Skibin: "High-frequency behavioral multiconductor cable modeling for EMI simulations in power electronics", *IEEE Trans. on Industrial Informatics*, Vol.10, No.2, pp.1392–1400 (2014)

(44) B. Wunsch, I. Stevanovic, and S. Skibin: "Length-scalable multiconductor cable modeling for EMI simulations in power electronics", *IEEE Trans. on Power Electronics*, Vol.32, No.3, pp.1908–1916 (2017)

(45) V.D. Santos, N. Roux, B. Revol, B. Sareni, B. Cougo, and J.P. Carayon: "Unshielded cable modeling for conducted emissions issues in electrical power drive systems", *2017 International Symposium on Electromagnetic Compatibility - EMC EUROPE*, pp.1–6 (2017)

(46) Y. Huangfu, L. Di Rienzo, and S. Wang: "Frequency-dependent multiconductor transmission line model for shielded power cables considering geometrical dissymmetry", *IEEE Trans. on Magnetics*, Vol.54, No.3, Article Sequence Number: 6300104 (2018)

(47) A. Consoli, G. Oriti, A. Testa, and A.L. Julian: "Induction motor modeling for common mode and differential mode emission evaluation", *IAS '96. Conference Record of the 1996 IEEE Industry Applications Conference Thirty-First IAS Annual Meeting*, pp.595–599 (1996)

(48) A. Boglietti and E. Carpaneto: "Induction motorhigh frequency model", *Conference Record of the 1999 IEEE Industry Applications Conference. Thirty-Forth IAS Annual Meeting*, pp.1551–1558 (1999)

(49) L. Wang, C.N. Ho, F. Canales, and J. Jatskevich: "High-frequency modeling of the long-cable-fed induction motor drive system using TLM approach for predicting overvoltage transients", *IEEE Trans. on Power Electronics*, Vol.25, No.10, pp.2653–2664 (2010)

(50) A. Boglietti, A. Cavagnino, and M. Lazzari: "Experimental high-frequency parameter identification of AC electrical motors", *IEEE Trans. on Industry Applications*, Vol.43, No.1, pp.23–29 (2007)

(51) N. Idir, Y. Weens, M. Moreau, and J.J. Franchaud: "High-frequency behavior models of AC motors", *IEEE Trans. on Magnetics*, Vol.45, No.1, pp.133–138 (2009)

(52) S. Maekawa, J. Tsuda, A. Kuzumaki, S. Matsumoto, H. Mochikawa, and H. Kubota: "EMI prediction method for SiC inverter by the modeling of structure and the accurate model of power device", *2014 International Power Electronics Conference* (*IPEC-Hiroshima 2014 - ECCE ASIA*), pp.1929–1934 (2014)

(53) P.R. Palmer, E. Santi, J.L. Hudgins, X. Kang, J.C. Joyce, and P.Y. Eng: "Circuit simulator models for the diode and IGBT with full temperature dependent features", *IEEE Trans. on Power Electronics*, Vol.18, No.5, pp.1220–1229 (2003)

(54) P.A.T. Bryant, X. Kang, E. Santi, P.R. Palmer, and J.L. Hudgins: "Two-step parameter extraction procedure with formal optimization for physics-based circuit simulator IGBT and p-i-n diode models", *IEEE Trans. on Power Electronics*, Vol.21, No.2, pp.295–309 (2006)

(55) A.T. Bryant, Y. Wang, S.J. Finney, T.C. Lim, and P.R. Palmer: "Numerical optimization of an active voltage controller for high-power IGBT converters", *IEEE Trans. on Power Electronics*, Vol.22, No.2, pp.374–383 (2007)

(56) A.T. Bryant, L. Lu, E. Santi, P.R. Palmer, and J.L. Hudgins: "Physical modeling of fast $p-i-n$ diodes with carrier lifetime zoning, part I: device model", *IEEE Trans. on Power Electronics*, Vol.23, No.1, pp.189–197 (2008)

(57) L. Lu, A.T. Bryant, E. Santi, P.R. Palmer, and J.L. Hudgins: "Physical modeling of fast $p-i-n$ diodes with carrier lifetime zoning, part II: parameter extraction", *IEEE Trans. on Power Electronics*, Vol.23, No.1, pp.198–205 (2008)

(58) A.T. Bryant, L. Lu, E. Santi, J.L. Hudgins, and P.R. Palmer: "Modeling of IGBT resistive and inductive turn-on behavior", *IEEE Trans. on Industry Applications*, Vol.44, No.3, pp.904–914 (2008)

(59) Y. Mukunoki, K. Konno, T. Matsuo, T. Horiguchi, A. Nishizawa, M. Kuzumoto, M. Hagiwara, and H. Akagi: "An improved compact model for a silicon-carbide MOSFET and its application to accurate circuit simulation", *IEEE Trans. on Power Electronics*, Vol.33, No.11, pp.9834–9842 (2018)

(60) Y. Mukunoki, Y. Nakamura, K. Konno, T. Horiguchi, Y. Nakayam, A. Nishizawa, M. Kuzumoto, and H. Akagi: "Modeling of a silicon-carbide MOSFET with focus on internal stray capacitances and inductances, and its verification", *IEEE Trans. on Industry Applications*, Vol.54, No.3, pp.2588–2597 (2018)

(61) L. Ran, S. Gokani, J. Clare, K.J. Bradley, and C. Christopulos: "Conducted electromagnetic emissions in induction motor drive systems part II: frequency domain models", *IEEE Trans. on Power Electronics*, Vol.13, No.4, pp.768–776 (1998)

(62) D. Gonzalez, J. Gago, and J. Balcells: "New simplified method for the simulation of conducted EMI generated by switched power converters", *IEEE Trans. on Industrial Electronics*, Vol.50, No.6, pp.1078–1084 (2003)

(63) X. Huang, E. Pepa, J.S. Lai, S. Chen, and T.W. Nehl: "Three-phase inverter differential mode EMI modeling and prediction in frequency domain", *38th IAS Annual Meeting on Conference Record of the Industry Applications Conference, 2003*, pp.2048–2055 (2003)

(64) F. Costa, C. Vollaire, and R. Meuret: "Modeling of conducted common mode perturbations in variable-speed drive systems", *IEEE Trans. on Electromagnetic Compatibility*, Vol.47, No.4, pp.1012–1021 (2005)

(65) X. Zhang, D. Boroyevich, P. Mattavelli, and F. Wang: "Filter design oriented EMI prediction model for DC-fed motor drive system using double fourier integral transformation method", *Proceedings of The 7th International Power Electronics and Motion Control Conference*, pp.1060–1064 (2012)

(66) C. Marlier, A. Videt, and N. Idir: "NIF-based frequency-domain modeling method of three-wire shielded energy cables for EMC simulation", *IEEE Trans. on Electromagnetic Compatibility*, Vol.57, No.1, pp.145–155 (2015)

(67) D. Drozhzhin, G. Griepentrog, A. Sauer, R. De Maglie, and A. Engler: "Suppression of conducted, high frequency signals in aerospace DC/AC converters designed with SiC MOSFETs", *2016 18th European Conference on Power Electronics and Applications* (*EPE'16 ECCE Europe*), pp.1–10 (2016)

(68) M. Foissac, J.L. Schanen, and C. Vollaire: ""Black box" EMC model for power electronics converter", *2009 IEEE Energy Conversion Congress and Exposition*, pp.3609–3615 (2009)

(69) M. Foissac, J.L. Schanen, G. Frantz, D. Frey, and C. Vollaire: "System simulation for EMC network analysis", *2011 Twenty-Sixth Annual IEEE Applied Power Electronics Conference and Exposition* (*APEC*), pp.457–462 (2011)

(70) H. Bishnoi, A.C. Baisden, P. Mattavelli, and D. Boroyevich: "Analysis of EMI terminal modeling of switched power converters", *IEEE Trans. on Power Electronics*, Vol.27, No.9, pp.3924–3933 (2012)

(71) G. Frantz, D. Frey, J.L. Schanen, H. Bishnoi, P. Mattavelli, and B. Revol: "EMC models for power electronics: from converter design to system level", *2013 IEEE Energy Conversion Congress and Exposition*, pp.4247–4252 (2013)

(72) G. Frantz, D. Frey, J.L. Schanen, and B. Revol: "EMC models of power electronics converters for network analysis", *2013 15th European Conference on Power Electronics and Applications* (*EPE*), pp.1–10 (2013)

(73) H. Bishnoi, P. Mattavelli, R. Burgos, and D. Boroyevich: "EMI behavioral models of DC-fed three-phase motor drive systems", *IEEE Trans. on Power Electronics*, Vol.29, No.9, pp.4633–4645 (2014)

(74) B. Sun and R. Burgos: "Assessment of switching frequency impact on the prediction capability of common-mode EMI emissions of SiC power converters using unterminated behavioral models", *2015 IEEE Applied Power Electronics Conference and Exposition* (*APEC*), pp.1153–1160 (2015)

(75) B. Sun, R. Burgos, X. Zhang, and D. Boroyevich: "Differential-mode EMI emission prediction of SiC-based power converters using a mixed-mode unterminated behavioral model", *2015 IEEE Energy Conversion Congress and Exposition* (*ECCE*), pp.4367–4374 (2015)

(76) H. Bishnoi, P. Mattavelli, R. Burgos, and D. Boroyevich: "EMI filter design of DC-fed motor-drives using behavioral EMI models", *2015 17th European Conference on Power Electronics and Applications* (*EPE'15 ECCE-Europe*), pp.1–10 (2015)

(77) D. Drozhzhin, G. Griepentrog, A. Sauer, R. De Maglie, and A. Engler: "Investigation on differential to common mode coupling in the output cable of AC drive for more electric aircraft", *2017 19th European Conference on Power Electronics and Applications* (*EPE'17 ECCE Europe*), pp.1–9 (2017)

(78) M. Amara, C. Vollaire, M. Ali, and F. Costa: "Black box EMC modeling of a three phase inverter", *2018 International Symposium on Electromagnetic Compatibility* (*EMC EUROPE*), pp.642–647 (2018)

(79) S. Shinde, K. Masuda, G. Shen, A. Patnaik, T. Makharashvili, D. Pommerenke, and V. Khilkevich: "Radiated EMI estimation from DC-DC converters with attached cables based on terminal equivalent circuit modeling", *IEEE Trans. on Electromagnetic Compatibility*, Vol.60, No.6, pp.1769–1776 (2018)

(80) A. Gahfif, P.E. Levy, M. Ali, M. Berkani, and F. Costa: "EMC "black box" model for unbalanced power electronic converters", *2019 International Symposium on Electromagnetic Compatibility* (*EMC EUROPE*), pp.957–962 (2019)

(81) F.Y. Shih, D.Y. Chen, Y.P. Wu, and Y.T. Chen: "A procedure for designing EMI filters for AC line applications", *IEEE Trans. on Power Electronics*, Vol.11, No.1, pp.170–181 (1996)

(82) J.W. Kolar, U. Drofenik, J. Biela, M. Heldwein, H. Ertl, T. Friedli, and S. Round: "PWM converter power density barriers", *IEEJ Trans. on Industry Applications*, Vol.128, No.4, pp.468–480 (2008)

(83) M.L. Heldwein and J.W. Kolar: "Impact of EMC filters on the power density of modern three-phase PWM converters", *IEEE Trans. on Power Electronics*, Vol.24, No.6, pp.1577–1588 (2009)

(84) T. Friedli, M. Hartmann, and J.W. Kolar: "The essence of three-phase PFC rectifier systems—part II", *IEEE Trans. on Power Electronics*, Vol.29, No.2, pp.543–560 (2014)

(85) K. Raggl, T. Nussbaumer, and J.W. Kolar: "Guideline for a simplified differential-mode EMI filter design", *IEEE Trans. on Industrial Electronics*, Vol.57, No.3, pp.1031–1040 (2010)

(86) D.O. Boillat, F. Krismer, and J.W. Kolar: "EMI filter volume minimization of a three-phase, three-level T-type PWM converter system", *IEEE Trans. on Power Electronics*, Vol.32, No.4, pp.2473–2480 (2017)

(87) B. Zaidi, A. Videt, and N. Idir: "Optimization method of CM inductor volume taking into account the magnetic core saturation issues", *IEEE Trans. on Power Electronics*, Vol.34, No.5, pp.4279–4291 (2019)

(88) F. Luo, S. Wang, F. Wang, D. Boroyevich, N. Gazel, Y. Kang, and A.C. Baisden: "Analysis of CM volt-second influence on CM inductor saturation and design for input EMI filters in three-phase DC-fed motor drive systems", *IEEE Trans. on Power Electronics*, Vol.29, No.2, pp.543–560 (2014)

(89) G. Ala, C. Giaconia, G. Giglia, M.C. Di Piazza, and G. Vitale: "Design and performance evaluation of a high power-density EMI filter for PWM inverter-fed induction-motor drives", *IEEE Trans. on Industry Applications*, Vol.52, No.3, pp.2397–2404 (2016)

(90) R. Chen, J.D. van Wyk, S. Wang, and W.G. Odendaal: "Improving the characteristics of integrated EMI filters by embedded conductive Layers", *IEEE Trans. on Power Electronics*, Vol.20, No.3, pp.611–619 (2005)

(91) J.D. van Wyk, F.C. Lee, Z. Liang, R. Chen, S. Wang, and B. Lu: "Integrating active, passive and EMI-filter functions in power electronics systems:a case study of some technologies", *IEEE Trans. on Power Electronics*, Vol.20, No.3, pp.523–536 (2005)

(92) J. Biela, A. Wirthmueller, R. Waespe, M.L. Heldwein, K. Raggl, and J.W. Kolar: "Passive and active hybrid integrated EMI filters", *IEEE Trans. on Power Electronics*, Vol.24, No.5, pp.1340–1349 (2009)

(93) M. Ali, E. Labouré, F. Costa, and B. Revol: "Design of a hybrid integrated EMC filter for a DC–DC power converter", *IEEE Trans. on Power Electronics*, Vol.27, No.11, pp.4380–4390 (2012)

(94) H. Huang, L. Deng, B. Hu, and G. Wei: "Techniques for Improving the high-frequency performance of the planar CM EMI filter", *IEEE Trans. on Electromagnetic Compatibility*, Vol.55, No.5, pp.901–908 (2013)

(95) M. Bartoli, A. Reatti, and M.K. Kazimierczuk: "Modelling iron-powder inductors at high frequencies", *Proceedings of 1994 IEEE Industry Applications Society Annual Meeting*, pp.1225–1232 (1994)

(96) A. Massarini, M.K. Kazimierczuk, and G. Grandi: "Lumped parameter models for single- and multiple-layer inductors", *PESC Record. 27th Annual IEEE Power Electronics Specialists Conference,* Baveno, pp.295–301 (1996)

(97) A. Roc'h, H. Bergsma, D. Zhao, B. Ferreira, and F. Leferink: "A new behavioural model for performance evaluation of common mode chokes", *2007 18th International Zurich Symposium on Electromagnetic Compatibility*, pp.501–504 (2007)

(98) M.L. Heldwein, L. Dalessandro, and J.W. Kolar: "The Three-Phase Common-Mode Inductor: Modeling and Design Issues", *IEEE Trans. on Industrial Electronics*, Vol.58, No.8, pp.3264–3274 (2011)

(99) C.R. Sullivan and A. Muetze: "Simulation model of common-mode chokes for high-power applications", *IEEE Trans. on Industry Applications*, Vol.46, No.2, pp.884–891 (2010)

(100) K. Nomura, N. Kikuchi, Y. Watanabe, S. Inoue, and Y. Hattori: "Novel SPICE model for common mode choke including complex permeability", *2016 IEEE Applied Power Electronics Conference and Exposition* (*APEC*),

pp.3146–3152 (2016)
(101) C. Cuellar, N. Idir, and A. Benabou: "High-frequency behavioral ring core inductor model", *IEEE Trans. on Power Electronics*, Vol.31, No.5, pp.3763–3772 (2016)
(102) K. Nomura, T. Kojima, and Y. Hattori: "Straightforward modeling of complex permeability for common mode chokes", *IEEJ Trans. on Industry Applications*, Vol.7, No.6, pp.462–472 (2018)
(103) B. Wunsch, S. Skibin, V. Forsstrom, and T. Christen: "Broadband modeling of magnetic components with saturation and hysteresis for circuit simulations of power converters", *IEEE Trans. on Magnetics*, Vol.54, No.11, Art no. 7301505, pp.1–5 (2018)
(104) S. Takahashi and S. Ogasawara: "A novel simulation model for common-mode inductors based on permeance-capacitance analogy", *2020 IEEE Energy Conversion Congress and Exposition* (*ECCE*), pp.5862–5869 (2020)
(105) A. Massarini and M.K. Kazimierczuk: "Self-capacitance of inductors", *IEEE Trans. on Power Electronics*, Vol.12, No.4, pp.671–676 (1997)
(106) G. Grandi, M.K. Kazimierczuk, A. Massarini, and U. Reggiani: "Stray capacitances of single-layer solenoid air-core inductors", *IEEE Trans. on Industry Applications*, Vol.35, No.5, pp.1162–1168 (1999)
(107) L. Dalessandro, F. da Silveira Cavalcante, and J.W. Kolar: "Self-capacitance of high-voltage transformers", *IEEE Trans. on Power Electronics*, Vol.22, No.5, pp.2081–2092 (2007)
(108) M. Kovacic, Z. Hanic, S. Stipetic, S. Krishnamurthy, and D. Zarko: "Analytical wideband model of a common-mode choke", *IEEE Trans. on Power Electronics*, Vol.27, No.7, pp.3173–3185 (2012)
(109) L. Middelstädt, S. Skibin, R. Döbbelin, and A. Lindemann: "Analytical determination of the first resonant frequency of differential mode chokes by detailed analysis of parasitic capacitances", *2014 16th European Conference on Power Electronics and Applications*, pp.1–10 (2014)
(110) S.W. Pasko, M.K. Kazimierczuk, and B. Grzesik: "Self-capacitance of coupled toroidal inductors for EMI filters", *IEEE Trans. on Electromagnetic Compatibility*, Vol.57, No.2, pp.216–223 (2015)
(111) A. Ayachit and M.K. Kazimierczuk: "Self-capacitance of single-layer inductors with separation between conductor turns", *IEEE Trans. on Electromagnetic Compatibility*, Vol.59, No.5, pp.1642–1645 (2017)
(112) S. Takahashi, S. Ogasawara, M. Takemoto, K. Orikawa, and M. Tamate: "A modeling technique for designing high-frequency three-phase common-mode inductors", *2018 IEEE Energy Conversion Congress and Exposition* (*ECCE*), pp.6600–6606 (2018)
(113) S. Wang, F.C. Lee, D.Y. Chen, and W.G. Odendaal: "Effects of parasitic parameters on EMI filter performance", *IEEE Trans. on Power Electronics*, Vol.19, No.3, pp.869–877 (2004)
(114) S. Wang, F.C. Lee, W.G. Odendaal, and J.D. van Wyk: "Improvement of EMI filter performance with parasitic coupling cancellation", *IEEE Trans. on Power Electronics*, Vol.20, No.5, pp.1221–1228 (2005)
(115) C. Cuellar and N. Idir: "Reduction of the parasitic couplings in the EMI filters to improve the high frequency insertion loss", *IECON 2018 - 44th Annual Conference of the IEEE Industrial Electronics Society*, pp.5766–5771 (2018)
(116) I.F. Kovačević, T. Friedli, A.M. Muesing, and J.W. Kolar: "3-D electromagnetic modeling of EMI input filters", *IEEE Trans. on Industrial Electronics*, Vol.61, No.1, pp.231–242 (2014)
(117) I.F. Kovačević, T. Friedli, A.M. Müsing, and J.W. Kolar: "3-D electromagnetic modeling of parasitics and mutual coupling in EMI filters", *IEEE Trans. on Power Electronics*, Vol.29, No.1, pp.135–149 (2014)
(118) A. Muetze: "Scaling issues for common-mode chokes to mitigate ground currents in inverter-based drive systems", *IEEE Trans. on Industry Applications*, Vol.45, No.1, pp.286–294 (2009)
(119) A. Muetze and C.R. Sullivan: "Simplified design of common-mode chokes for reduction of motor ground currents in inverter drives", *IEEE Trans. on Industry Applications*, Vol.47, No.6, pp.2570–2577 (2011)
(120) A. Roc'h and F. Leferink: "Nanocrystalline core material for high-performance common mode inductors", *IEEE Trans. on Electromagnetic Compatibility*, Vol.54, No.4, pp.785–791 (2012)
(121) M. Kącki, M.S. Rylko, J.G. Hayes, and C.R. Sullivan: "Magnetic material selection for EMI filters", *2017 IEEE Energy Conversion Congress and Exposition* (*ECCE*), pp.2350–2356 (2017)
(122) D. Han, C.T. Morris, W. Lee, and B. Sarlioglu: "Comparison between output CM chokes for SiC drive operating at 20- and 200-kHz switching frequencies", *IEEE Trans. on Industry Applications*, Vol.53, No.3, pp.2178–2188 (2017)
(123) D.A. Rendusara and P.N. Enjeti: "An improved inverter output filter configuration reduces common and differential modes dv/dt at the motor terminals in PWM drive systems", *IEEE Trans. on Power Electronics*, Vol.13, No.6, pp.1135–1143 (1998)
(124) H. Akagi, H. Hasegawa, and T. Doumoto: "Design and performance of a passive EMI filter for use with a voltage-source PWM inverter having sinusoidal output voltage and zero common-mode voltage", *IEEE Trans. on Power Electronics*, Vol.19, No.4, pp.1069–1076 (2004)
(125) H. Akagi and T. Doumoto: "An approach to eliminating high-frequency shaft voltage and ground leakage current from an inverter-driven motor", *IEEE Trans. on Industry Applications*, Vol.40, No.4, pp.1162–1169 (2004)
(126) H. Akagi and T. Doumoto: "A passive EMI filter for preventing high-frequency leakage current from flowing through the grounded inverter heat sink of an adjustable-speed motor drive system", *IEEE Trans. on Industry Applications*, Vol.41, No.5, pp.1215–1223 (2005)
(127) H. Akagi and S. Tamura: "A passive EMI filter for eliminating both bearing current and ground leakage current from an inverter-driven motor", *IEEE Trans. on Power Electronics*, Vol.21, No.5, pp.1459–1469 (2006)
(128) H. Akagi and T. Oe: "A specific filter for eliminating high-frequency leakage current from the grounded heat sink in a motor drive with an active front end", *IEEE Trans. on Power Electronics*, Vol.23, No.2, pp.763–770 (2008)
(129) H. Akagi and T. Shimizu: "Attenuation of conducted EMI emissions from an inverter-driven motor", *IEEE Trans. on Power Electronics*, Vol.23, No.1, pp.282–290 (2008)
(130) M.M. Swamy, K. Yamada, and T. Kume: "Common mode current attenuation techniques for use with PWM drives", *IEEE Trans. on Power Electronics*, Vol.16, No.2, pp.248–255 (2001)
(131) X. Chen, D. Xu, F. Liu, and J. Zhang: "A novel inverter-output passive filter for reducing both differential- and common-mode dv/dt at the motor terminals in PWM drive systems", *IEEE Trans. on Industrial Electronics*, Vol.54, No.1, pp.419–426 (2007)
(132) S. Ohara, S. Ogasawara, M. Takemoto, K. Orikawa, and Y. Yamamoto: "A hybrid common-mode voltage cancellation using a passive filter and an active feedback circuit for PWM inverters", *2019 IEEE 4th International Future Energy Electronics Conference* (*IFEEC*), pp.1–6 (2019)
(133) S. Ogasawara, H. Ayano, and H. Akagi: "An active circuit for cancellation of common-mode voltage generated by a PWM inverter", *IEEE Trans. on Power Electronics*, Vol.13, No.5, pp.835–841 (1998)
(134) M.C. Di Piazza, G. Tine, and G. Vitale: "An improved active common-mode voltage compensation device for induction motor drives", *IEEE Trans. on Industrial Electronics*, Vol.55, No.4, pp.1823–1834 (2008)
(135) S. Ohara, S. Ogasawara, T. Masatsugu, K. Orikawa, and Y. Yamamoto: "A novel active common-noise canceler combining feedforward and feedback control", *2017 IEEE Energy Conversion Congress and Exposition* (*ECCE*), pp.2469–2475 (2017)
(136) I. Takahashi, A. Ogata, H. Kanazawa, and A. Hiruma: "Active EMI filter for switching noise of high frequency inverters", *Proceedings of Power Conversion Conference - PCC '97*, pp.331–334 (1997)
(137) Y.C. Son and S.K. Sul: "Conducted EMI in PWM inverter for household electric appliance", *IEEE Trans. on Industry Applications*, Vol.38, No.5, pp.1370–1379 (2002)
(138) Y.C. Son and S.K. Sul: "A new active common-mode EMI filter for PWM inverter", *IEEE Trans. on Power Electronics*, Vol.18, No.6, pp.1309–1314 (2003)
(139) M. Zhu, D.J. Perreault, V. Caliskan, T.C. Neugebauer, S. Guttowski, and J.G. Kassakian: "Design and evaluation of feedforward active ripple filters", *IEEE Trans. on Power Electronics*, Vol.20, No.2, pp.276–285 (2005)
(140) Y.C. Son and S.K. Sul: "Generalization of active filters for EMI reduction and harmonics compensation", *IEEE Trans. on Industry Applications*, Vol.42, No.2, pp.545–551 (2006)
(141) S. Wang, Y.Y. Maillet, F. Wang, D. Boroyevich, and R. Burgos: "Investigation of hybrid EMI filters for common-mode EMI suppression in a motor drive system", *IEEE Trans. on Power Electronics*, Vol.25, No.4, pp.1034–1045 (2010)
(142) P. Cantillon-Murphy, T.C. Neugebauer, C. Brasca, and D.J. Perreault: "An active ripple filtering technique for improving common-mode inductor performance", *IEEE Power Electronics Letters*, Vol.2, No.2, pp.45–50 (2004)
(143) K. Mainali and R. Oruganti: "Design of a current-sense voltage-feedback common mode EMI filter for an off-line power converter", *IEEE Power Electronics Specialists Conference*, pp.1632–1638 (2008)
(144) W. Chen, X. Yang, and Z. Wang: "An active EMI filtering technique for improving passive filter low-frequency performance", *IEEE Trans. on Electromagnetic Compatibility*, Vol.48, No.1, pp.172–177 (2006)
(145) M. Li, M. Shen, L. Xing, and W. Said: "Current feedback based hybrid common-mode EMI filter for grid-tied inverter application", *IEEE Energy Conversion Congress and Exposition* (*ECCE*), pp.1394–1398 (2012)
(146) D. Hamza and P.K. Jain: "Conducted EMI noise mitigation in DC-DC converters using active filtering method", *2008 IEEE Power Electronics Specialists Conference*, pp.188–194 (2008)
(147) M.C. Di Piazza, A. Ragusa, and G. Vitale: "An optimized feedback common mode active filter for vehicular induction motor drives", *IEEE Trans. on Power Electronics*, Vol.26, No.11, pp.3153–3162 (2011)

(148) M. Ali, E. Labouré, and F. Costa: "Integrated active filter for differential-mode nise suppression", *IEEE Trans. on Power Electronics*, Vol.29, No.3, pp.1053–1057 (2014)

(149) M.L. Heldwein, H. Ertl, J. Biela, and J.W. Kolar: "Implementation of a transformerless common-mode active filter for offline converter systems", *IEEE Trans. on Industrial Electronics*, Vol.57, No.5, pp.1772–1786 (2010)

(150) S. Takahashi, S. Ogasawara, M. Takemoto, K. Orikawa, and M. Tamate: "An active common-mode filter for reducing radiated noise from power cables", *IEEE 3rd International Future Energy Electronics Conference and ECCE Asia* (*IFEEC 2017 - ECCE Asia*), pp.1753–1758 (2017)

(151) S. Takahashi, S. Ogasawara, M. Takemoto, K. Orikawa, and M. Tamate: "A study on reduction techniques of a wideband common-mode voltage produced by a PWM inverter", *International Power Electronics Conference* (*IPEC-Niigata 2018 -ECCE Asia*), pp.3315–3322 (2018)

(152) S. Takahashi, S. Ogasawara, M. Takemoto, K. Orikawa, and M. Tamate: "Common-mode voltage attenuation of an active common-mode filter in a motor drive system fed by a PWM inverter", *IEEE Trans. on Industrial Applications*, Vol.55, No.3, pp.2721–2730 (2019)

Shotaro Takahashi (Member) received Dr.Eng. degree from Hokkaido University, Sapporo, Hokkaido, Japan in March 2020. From April 2020 to March 2021, He was a project assistant professor in Tokyo Metropolitan University, Hachioji, Tokyo, Japan. Currently, He has been an assistant professor with Seikei University, Kichijoji, Tokyo, Japan since April 2021. His current research focuses on electromagnetic compatibility of high-frequency switching power converters, active electromagnetic interference filters, and modeling of magnetic components. He is a member of IEICE and IEEE.

Keiji Wada (Senior Member) received a Ph.D. degree in electrical engineering from Okayama University, Japan, in 2000. From 2000 to 2006, he was an assistant professor with Tokyo Metropolitan University and the Tokyo Institute of Technology. He became an associate professor in 2006 and a professor in 2021 at Tokyo Metropolitan University. His current research interests include gate-drive circuits, electromagnetic interference filters, and a power converter circuit. He is a senior member of IEEE.

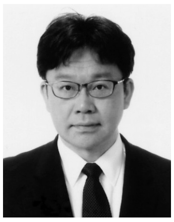

Hideki Ayano (Senior Member) received the B.S. and M.S. degrees in electrical and electric engineering from Okayama University, Okayama, Japan, in 1995 and 1997, respectively. In 1997, he was with Hitachi, Ltd. He received Dr.Eng. Degree in electrical engineering from Utsunomiya University, Tochigi, Japan in 2006. Since 2011, he has been with the National Institute of Technology, Tokyo College, where he is currently a professor. His research interests include power converters, motor drive, electromagnetic interference problems, etc. He is a Senior Member of the IEEE and a Senior Member of the Institute of Electrical Engineers of Japan.

Satoshi Ogasawara (Fellow) received B.S., M.S., and Dr.Eng. Degrees in electrical engineering from the Nagaoka University of Technology, Japan, in 1981, 1983, and 1990, respectively. From 1983 to 1992, he was a Research Assosiate at Nagaoka University of Technology. From 1992 to 2003, he has with the Department of Electrical Engineering, Okayama University, Japan. From 2003 to 2007, he was with the Department of Electrical Engineering, Utsunomiya University, Japan. Since 2007, he has been a Professor in the Graduate School of Information Science and Technology, Hokkaido University, Japan. His research interest include AC motor drive systems and static power converters. He is a senior member of IEEE and a fellow of IEEJ.

Toshihisa Shimizu (Fellow) received the B.E., M.E., and Dr.Eng. degrees in electrical engineering from Tokyo Metropolitan University, Tokyo, Japan, in 1978, 1980, and 1991, respectively. In 1998, he was a Visiting Professor at the Virginia Power Electronics Center, Virginia Polytechnic Institute and State University, Blacksburg, VA, USA. He joined Fuji Electric Corporate Research and Development Ltd., in 1980. Since 1993, he has been with the Department of Electrical Engineering, Tokyo Metropolitan University, Tokyo, where he is currently a Professor Emeritus. He has authored or co-authored more than 70 journal papers and 120 international conference proceedings, and six technical books. He also holds 10 patents and has more than 10 patents pending. His current research interests include power converters, high-frequency inverters, photovoltaic power generations, uninterruptible power supplies, electromagnetic interference problems, high power density converter design, inductor loss analysis, etc. Dr. Shimizu is an Associate Editor for the Transactions on Power Electronics. He was the recipient of Transactions Paper Awards from the Institute of Electrical Engineers of Japan in 1999 and 2010, two Best Paper Awards from the 2010 International Power Electronics Conference—ECCE Asia, and a Best Paper Award from the International Power Electronics and Motion Control Conference. He is a fellow of IEEE and IEEJ.